

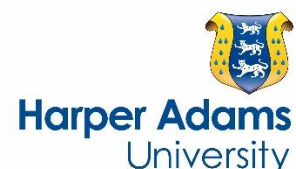
# The evaluation and calibration of pressure mapping system for the measurement of the pressure distribution of agricultural tyres

by Misiewicz, P.A. , Blackburn, K., Richards, T.E., Brighton, J.L. and Godwin, R.J.

**Copyright, Publisher and Additional Information:** This is the author accepted manuscript. The final published version (version of record) is available online via Elsevier

Please refer to any applicable terms of use of the publisher.

DOI: [10.1016/j.biosystemseng.2014.12.006](https://doi.org/10.1016/j.biosystemseng.2014.12.006)



Misiewicz, P.A. , Blackburn, K., Richards, T.E., Brighton, J.L. and Godwin, R.J. 2015. The evaluation and calibration of pressure mapping system for the measurement of the pressure distribution of agricultural tyres. *Biosystems Engineering*. 130, 81-91.

1 **The evaluation and calibration of pressure mapping system for**  
2 **the measurement of the pressure distribution of agricultural tyres**  
3

4 P. A. Misiewicz<sup>a, 1</sup>, K. Blackburn<sup>a</sup>, T. E. Richards<sup>a</sup>, J. L. Brighton<sup>a</sup> and R. J. Godwin<sup>a, 1</sup>  
5

6 <sup>a</sup>Cranfield University, Cranfield, Bedfordshire, MK43 0AL, UK

7 <sup>1</sup>Harper Adams University, Newport, TF10 8NB, UK  
8

9 Corresponding author: [p.misiewicz@iagre.biz](mailto:p.misiewicz@iagre.biz); +44 7752 954149  
10

11 **Abstract**

12 The accuracy of a commercial pressure mapping system was evaluated and a number of  
13 techniques for the improvement of pressure measurements were developed. These were  
14 required in order to use the pressure mapping system in a tyre/surface interaction study which  
15 involved determination of the tyre contact pressure distribution on, both, hard and soil  
16 surfaces. In the evaluation of the system, the effect of sensor calibration procedures on the  
17 accuracy of the system in measuring pressure was investigated. A purpose built pressure  
18 calibration chamber was used to calibrate the sensors, which enabled the proprietary built-in  
19 calibration system to be evaluated along with a novel calibration procedure employing, both,  
20 an individual and multi-point calibration of each sensing element and the rejection of sensing  
21 elements that did not conform to the sensitivity of the majority of the sensing elements.  
22 These measures reduced the uncertainty in pressure measurements from  $\pm 30\%$  to  $\pm 4\%$ .  
23 Further, evaluation of the compliance of the material was also conducted to enable the  
24 sensors to be used for interface pressure measurements between two different surface  
25 materials other than those used during sensor calibration. As a result, a procedure for  
26 normalising the recorded pressure by adjusting the recorded load output to equal the applied  
27 load was established. The improvement of the accuracy of the sensors made it possible for  
28 the system to be used to determine the pressure distribution resulting from a range of tyres on  
29 a hard surface and in the soil profile.  
30

31 **Keywords:** pressure mapping system; calibration; contact pressure; soil – tyre interactions.  
32  
33  
34

35 **1 Introduction**

36 Over the last few decades, farm machinery has increased substantially in weight, increasing  
37 loads on the soil and exacerbating compaction problems (Horn, Fleige, Peth, & Peng, 2006).  
38 As wheel traffic results in soil compaction (Soane and Ouwerkerk, 1994), a better  
39 understanding of soil contact pressure and load transfer to soil through agricultural tyres is  
40 essential to provide improved solutions to tyre selection. There is, therefore, a need for an  
41 accurate tyre contact pressure measurement system. This article reports on the selection and  
42 performance enhancement of a commercial pressure mapping system.

43  
44 Misiewicz (2010) conducted a review of the commercially available pressure mapping  
45 systems, where sensor flexibility, size, pressure resolution, ability to upgradeable the system,  
46 customisability, reuse, static vs. dynamic application, test-monitoring capability, modularity  
47 and cost were considered. The Tekscan system, I-Scan and Conformat versions (Tekscan,  
48 Inc. South Boston, Mass., USA), based on piezo-electric pressure sensors, which enable real-  
49 time contact area and pressure distribution to be measured across a multi-sensor array over  
50 time (Tekscan, not dated a), was selected for this study due to the sensor size and pressure  
51 resolution required to measure the pressure distribution below agricultural tyres. The system  
52 measures the load applied to each sensing element and records it as the interface pressure  
53 between two surfaces. Tekscan sensors contain thin sensing mats built as a multi-sensor  
54 array varying in size, shape, spatial resolution and pressure range. The system contains: (a)  
55 piezo-electric pressure sensitive mats (called sensors), (b) data acquisition handle (adaptor)  
56 that communicates through a USB interface, (c) data acquisition software and (d) a sensor  
57 software map. The system has a wide range of pressure measurement applications including  
58 the medical, automotive and furniture design industries. The Tekscan system has an 8-bit  
59 output, where each individual sensing element (called a sensel) has a resolution of 0.4% of  
60 the full scale output. The thin construction of the sensors allows them to be deformed and  
61 permits minimally intrusive/invasive surface pressure measurements (Tekscan, not dated b).

62  
63 Before the sensor is used, it should be calibrated to convert its output into engineering units  
64 and the output variations between individual sensing elements of any given sensor minimised  
65 by applying a uniform pressure across the entire sensor; this process is called equilibration  
66 (Tekscan, 2006). There have been a number of studies investigating aspects of the Tekscan  
67 system accuracy in determining contact pressure and area of contact (Drewniak, Crisco,  
68 Spenciner, & Fleming, 2007). Sumiya, Suzuki, Kasahara, and Ogata (1998) concluded that

69 the Tekscan system does not measure the normal pressures accurately enough for a high level  
70 of certainty in terms of absolute values, but it does enable relative comparisons of pressure  
71 distribution to be made. Problems of pressure drift, repeatability, linearity and hysteresis  
72 were evaluated by Ferguson-Pell, Hagusawa, and Bain (2000) and Wilson, Niosi, Zhu,  
73 Oxland, and Wilson (2006), who stressed the importance of calibration to minimise the  
74 system errors.

75  
76 A number of studies have evaluated the effect of the calibration procedure on the accuracy of  
77 the system. The proprietary software has two built-in calibration functions, (i) one-point  
78 linear and (ii) two-point power calibrations, both with an assumption that zero force equals  
79 zero output. These calibrations are conducted by applying a known uniform load to the entire  
80 previously equilibrated sensor (Tekscan, 2006). Wilson et al. (2006) and Wilson, Apreleva,  
81 Eichler, and Harrold (2003) found that measurements made using a linear calibration were  
82 more repeatable and accurate than those made with a two-point power calibration, however,  
83 studies conducted by Brimacombe, Anglin, Hodgson, and Wilson (2005) contradicted this  
84 finding and showed that the power calibration of the sensors gave significantly lower errors  
85 of 2.7%, in comparison to 24.4% and 10.5% obtained for two linear calibrations conducted at  
86 20% and 80% of the maximum load, respectively. Further, their study developed user-  
87 defined 3-point quadratic and 10-point cubic calibrations, which were found to further reduce  
88 the errors associated with the power calibration to 1.5% and 0.6%, respectively. Similar  
89 results were found by DeMarco, Rust, and Bachus (2000). These studies, however,  
90 conducted the evaluation of sensor entire output without any consideration given to the  
91 output of individual sensing elements.

92  
93 The previous studies evaluating sensor performance point out the importance of the  
94 appropriate calibration of the sensors in order to reduce the uncertainties in the results. This  
95 study evaluates the proprietary built-in Tekscan calibration and development of a novel  
96 polynomial 'per sensel' calibration and its ability to reduce the errors associated with the  
97 pressure determination of individual elements. In order to do so, the following methodology  
98 was established:

- 99 (i) The design and construction of a novel pressure calibration device,
- 100 (ii) The evaluation of the Tekscan proprietary calibration,
- 101 (iii) The development and evaluation of a calibration procedure for each sensel with 10  
102 predetermined pressures applied over the operating range where the non-

103 responsive sensels were disregarded; referred in the following as ‘multi-point per  
104 sensel calibration with sensel selection’, and

105 (iv)The correction of the multi-point per sensel calibration with sensel selection.

106 This was conducted in order to determine an effective method to measure the pressure  
107 distribution below pneumatic agricultural tyres on both hard surfaces and within the soil  
108 profile (Misiewicz, 2010).

109

## 110 **2 The design and construction of a novel pressure calibration chamber**

111 Each Tekscan sensor needs to be equilibrated and calibrated before being used for pressure  
112 measurements; five Tekscan sensors were selected for this study, equilibrated and calibrated  
113 using a purpose-built pressure calibration chamber. The calibration of the sensors was  
114 conducted by two methods; firstly, the sensors were equilibrated and calibrated following the  
115 guidelines from Tekscan (Tekscan, 2006). The second method involved the development of  
116 a novel calibration procedure where each sensing element was calibrated separately using the  
117 multi-point data procedure. An evaluation of the accuracy of the sensors was conducted after  
118 the sensors were calibrated and equilibrated.

119

120 The following Tekscan sensors, shown in Fig. 1, were selected, as their size, shape and  
121 pressure range were the most suitable for the tyre contact pressure study by Misiewicz  
122 (2010):

- 123 • Conformat system: Model 5330 sensor
  - 124 - standard pressure range: 0 -  $0.55 \times 10^5$  Pa
  - 125 - sensor dimensions: 471.4 mm x 471.4 mm
  - 126 - number of sensing elements: 1024
- 127 • I-Scan system: Model 6300-A and 6300-B sensors
  - 128 - standard pressure range: 0 -  $3.45 \times 10^5$  Pa
  - 129 - sensor dimensions: 264.2 mm x 33.5 mm
  - 130 - number of sensing elements: 2288
- 131 • I-Scan system: Model 9830-A and 9830-B sensors
  - 132 - standard pressure range: 0 -  $0.7 \times 10^5$  Pa
  - 133 - sensor dimensions: 188.6 mm x 203.2 mm
  - 134 - number of sensing elements: 176

135 The standard pressure range of each sensor can be increased or decreased by a factor of 10  
136 using the appropriate software scaling function.

137  
138 In order to provide a fundamental and independent calibration of the Tekscan sensors, a  
139 calibration chamber was designed and constructed to allow the application of uniform  
140 pneumatic pressure to all sensing elements being simultaneously calibrated (Misiewicz,  
141 2010). The calibration system consisted of a lower and upper plate, as shown in [Figure-Fig. 2](#)  
142 and [Figure-Fig. 3](#). A Tekscan sensor was placed on the smooth ground upper surface of the  
143 bottom plate and then a diaphragm placed on the sensor followed by the top plate. The two  
144 plates were bolted together by 28 M16 set-screws. Pressure was applied inside the device  
145 from the top into the plenum chamber and recorded using a digital pressure gauge (range of 0  
146 –  $20 \times 10^5$  Pa). The system was designed for a maximum safe working pressure of  $34.5 \times 10^5$   
147 Pa. Air can be used to pressurise the device up to  $8 \times 10^5$  Pa, whilst oil is recommended for  
148 pressures above  $8 \times 10^5$  Pa. Depending on the pressure range, a flexible rubber or polythene  
149 membrane was used as the diaphragm to seal the device whilst allowing a uniform pressure  
150 application to the entire sensor. The entire system weighed 0.28 t.

151

### 152 **3 Evaluation of the Tekscan proprietary calibration**

153 Following the manufacturer's recommendations to reduce the effect of drift and hysteresis  
154 (Tekscan, 2006), each sensor was conditioned by repeatedly applying air pressure five times,  
155 before it was calibrated. Sensors were loaded with uniform pressure to values approximately  
156 20% greater than those expected during the studies. For the equilibration and calibration air  
157 pressure was applied to the sensor as follows:

158 1) The equilibration was conducted in 10 increments when pressure was increased. Prior  
159 to this process a minimum pressure of  $0.1 \times 10^5$  Pa was applied to the sensor for one minute  
160 to establish an equilibrium condition.

161 2) During the calibration process, a scale factor established during the equilibration  
162 process was applied by the proprietary software to each sensing element to make the output  
163 uniform between sensels. A two-point calibration was performed by applying two different  
164 pressures to the sensor (20% and 80% of the expected maximum pressure). The pressures  
165 were applied for one second to allow the pressure to stabilise. Using these data a power law  
166 interpolation for overall sensor based on zero load and the two known calibration loads was  
167 performed.

168

169 Based on the proprietary calibration, the mean, maximum and minimum pressures were  
170 determined for each sensor and compared to the applied pressures measured by the air  
171 pressure gauge, as shown in Table 1. The bias errors of the overall sensel pressures were less  
172 than 3.0% for the Conformat 5300, I-Scan 6300-A and 6300-B sensors; the I-Scan 9830-A  
173 and 9830-B produced bias errors as high as 12.5%.

174  
175 ~~Figure-Fig.~~ 4 presents a series of histograms of the residual errors obtained when the sensors  
176 were pressurised with uniform pressure. Each histogram presents all the errors obtained for  
177 the sensels of the sensor tested at the range of applied pressures. Several outliers were found  
178 for each sensor, which give evidence of the presence of “erroneous” sensels. The histograms  
179 show that the I-Scan 6300-A, 6300-B, 9830-A and 9830-B gave residual errors up to  $\pm 30\%$   
180 nearly normally distributed around “0”. The Conformat 5330 was found to have a tendency  
181 to record a higher-than-applied pressure with the errors below 10%. This illustrates that the  
182 Tekscan sensors calibrated using the proprietary software give acceptable errors of the mean  
183 pressure with some sensels giving large variations in the pressure distribution up to 30%.

184  
185 As shown by Misiewicz (2010), the entire area of Conformat 5330 provided errors below  
186 10%, and 98% of the area gave errors less than 5%. However, the other four sensors were  
187 generally associated with larger errors and only 92% – 98% of the sensing area gave errors  
188 less than a 10% error, and 64% – 86% of the area had errors less than 5%.

189  
190 Following calibration and equilibration using the Tekscan calibration procedure experiments  
191 involving rolling loaded tyres over the sensors on a hard surface were conducted. The data  
192 were collected by the two I-Scan 9830 sensors, which overlapped the tyre centre line by 50  
193 mm. Figure 5 illustrates contact pressure profiles (cross-sections) found below the centre of  
194 a smooth (with the tread removed) Trelleborg T421 Twin Implement 600/55-26.5 tyre. The  
195 raw outputs collected by the two sensors from the overlapping area, plotted in Fig. 5a, were  
196 found to be similar. When the Tekscan proprietary calibration and equilibration were applied  
197 to the data, the results were found to differ significantly by up to 26% (Fig. ~~4~~ 5b). Hence,  
198 the results shown in Fig. 5 confirm a requirement for an evaluation of data modification  
199 protocols associated with the proprietary calibration and equilibration, and a requirement for  
200 an improved calibration protocol.

201

202 To understand the raw output (non-calibrated and non-equilibrated) and the functions that are  
203 applied to the data by the Tekscan software, the raw data were collected and analysed. As the  
204 Tekscan calibration procedure involves establishing one regression curve for an entire sensor,  
205 which is an average value for all the sensing elements, it was necessary to verify the raw  
206 output data of each individual sensel in order to determine if they had similar characteristics.

207  
208 In order to do this the sensors were placed in the calibration chamber and air pressure was  
209 applied. Both, the raw output data (non-calibrated and non-equilibrated) and equilibrated  
210 data recorded, were plotted against the applied pressure, as shown for the I-Scan 9830-A  
211 sensor in Fig. 6. The data were plotted using the proprietary convention for calibration, to  
212 enable the pressure to be readily determined from the Tekscan output in the form of the  
213 equations given. Figure 6 shows how the Tekscan equilibration function modifies the results.  
214 Plotting the data has verified that the output characteristic varied between the sensels,  
215 however, the equilibration procedure was found to account for the different calibration  
216 characteristics to a great extent. Best-fit power functions were established to visualise the  
217 differences in the sensor performance. After the equilibration was applied to the raw output,  
218 the maximum variation was found to decrease from 130% to 6%. This agrees with findings  
219 of Maurer et al. (2003), who proved that sensor equilibration, which accounts for variations  
220 between the individual sensing elements of a sensor, is effective in reducing inter-cell  
221 variations.

222  
223 The evaluation of the raw data showed the variations between the individual sensing elements  
224 of a sensor and the importance of equilibration in reducing these variations. This confirmed a  
225 need for a multi-point calibration of all the sensors and a separate consideration of each  
226 sensing element during the calibration to account for the equilibration of sensors.

#### 228 **4 The development and evaluation of the multi-point per sensel calibration with** 229 **sensel selection**

230 The second method of calibrating the sensors involved directly recording the raw values  
231 available from the Tekscan system when applying a number of air pressures to the sensels in  
232 increasing increments. This was conducted in order to establish a multi-point calibration for  
233 each individual sensing element and to locate the sensors giving no output or values that were  
234 in excess of the expected range.

235



236 Before calibrating the sensors, they were conditioned by repeatedly (x5) applying a uniform  
237 pressure to values approximately 20% greater than those expected during the tests. Then the  
238 multi-point calibration was conducted, this involved an application of air pressure across the  
239 sensor in 10 increasing increments from 10% to 100% of the maximum pressure expected for  
240 each sensor. Each pressure was applied for one second and the raw data recorded and  
241 processed in order to establish linear, power, second, third and fourth order polynomial  
242 relationships. They were then used for the evaluation of the multi-point per sensel  
243 calibration. The identification of erroneous and non-responsive sensels was required in order  
244 to eliminate them before the calibration constants were applied. The de-selection was based  
245 on the following criteria:

- 246 • non-responsive sensels: the sensels giving zero output when loaded,
- 247 • erroneous sensels: visual selection of outliers.

248

249 The data obtained for the 9830-A sensor were selected for evaluation of the multi-point per  
250 sensel calibration, as this sensor was the most appropriate for the experimental work of  
251 Misiewicz (2010). The residual errors were plotted as histograms for each type of regression  
252 curve and are shown in Fig. 7. The results showed that the design of the multi-point per  
253 sensel calibration significantly improved the accuracy of the pressure measurements by  
254 reducing the bias errors below 1%. The residual errors were found to be below 7% for the  
255 linear calibration, below 5% for the 2<sup>nd</sup> order polynomial calibration and below 4% for the 3<sup>rd</sup>  
256 and 4<sup>th</sup> order polynomials. The power function was found to have the least effect in reducing  
257 the errors, as the residuals were found to vary from -10% to +20%. Therefore, the findings  
258 confirmed that the polynomial functions give the closest fit to the data and improve the  
259 accuracy of the system.

260

261 As shown by Misiewicz (2010), the polynomial regression curves gave the best accuracy of  
262 the data for the 9830-A sensor with the 4<sup>th</sup> order polynomial providing residual errors below  
263 3% for all sensing elements of the sensor and 88% of the elements giving errors below 1%.  
264 In the case of the linear regression, 99% of the sensor area provided errors below 5% and  
265 only 51% was associated with errors less than 1%. The power function provided the greatest  
266 residual errors, with 71% of the area having errors less than 3% and only 32% of the area had  
267 errors less than 1%.

268

269 In order to further check the accuracy of the multi-point calibration, sets of raw data were  
270 obtained by loading the 9830-A sensor with air pressure in the calibration chamber with a  
271 previously established multi-point calibration applied to the data. The statistical errors of  
272 individual sensing elements were calculated and presented in Fig. 8. Generally, the results  
273 were found to slightly underestimate the pressures and the highest statistical errors were  
274 found again for the power function, which varied from  $-10\%$  to  $+3\%$ . For the linear  
275 relationships the errors varied from  $-7\%$  and  $+3\%$ . For the 2<sup>nd</sup>, 3<sup>rd</sup> and 4<sup>th</sup> order polynomials  
276 the errors were the smallest, varying between  $-3\%$  and  $+2\%$ .

277  
278 The polynomial models give the largest amount of sensing area of the 9830- sensor with  
279 small errors; for the 2<sup>nd</sup> and 3<sup>rd</sup> order polynomial almost 100% of the sensor area was  
280 associated with statistical errors lower than 3% and 60% of the area had errors lower than  
281 1%. The 4<sup>th</sup> order polynomial function gave slightly improved results as 100% and 67% of  
282 the sensing area had statistical errors lower than 3% and 1%, respectively, while for the linear  
283 and power functions only 32% and 30% of the area gave errors smaller than 1%, and 80%  
284 and 60% gave errors smaller than 3% (Misiewicz, 2010).

285  
286 The evaluation of the performance of sensors calibrated using the multi-point per sensel  
287 calibration with sensel selection was found to improve the accuracy of the results (below  ~~$\pm 4\%$~~   
288 4%), although there were still some residual variations but they were lower than the  
289 variations obtained following the proprietary recommended calibration (up to  $\pm 30\%$ ).

290

## 291 **5 The correction of the multi-point per sensel calibration with sensel selection**

292 Tekscan sensors have a varied output that depends on the materials used to apply the pressure  
293 to the sensor (Tekscan, 2006). The sensors consist of active and non-active areas and the  
294 load applied to the active area of each sensel is measured. An assumption made regarding the  
295 system is that the same load is applied to the non-active area and the system determines the  
296 pressure as the total load over the sensel area. Hence, the flexibility of the material that is in  
297 contact with the sensor plays an important role in pressure transfer. It can be assumed that  
298 for the highest levels of accuracy, Tekscan sensors should be calibrated with exactly the same  
299 interface material as the one used during testing. Unfortunately this is not always possible.  
300 In this study, during the calibration, a sensor was placed on the smooth ground surface of a  
301 steel plate; a flexible rubber or polythene diaphragm was then placed over the sensor. Air  
302 pressure was uniformly applied to the diaphragm. In the tyre contact pressure study of

303 Misiewicz (2010), both, the hard surface and soil experiments, involved a smooth aluminium  
304 plate loaded by a pneumatic tyre and Tekscan sensor placed at the interface either directly or  
305 through the soil. Materials with similar characteristics were used in both the calibration and  
306 experiments. The rubber and polythene membrane, used in the calibration process, were  
307 expected to distribute the pressure in a manner similar to a pneumatic tyre. This was  
308 evaluated by comparing the total load applied to the tested tyres and the total load recorded  
309 by Tekscan sensors. In case of a poor agreement, a correction factor would need to be  
310 developed to account for the compliance of different interface materials and to enable the  
311 system to provide pressure measurements between different surface interfaces.

312

313 In order to evaluate the requirement for a correction factor, two sets of experiments were  
314 conducted. These were as follows:

315 a. A comparison of the calibration and test environments in a small scale controlled  
316 study

317 This was conducted using the I-Scan 9830 sensors as they were selected, as being those that  
318 might produce the greatest discrepancy due to a relatively low spatial resolution of sensels  
319 (active area of each sensel: 6.3 mm x 3.8 mm). Initially a multi-point per sensel calibration  
320 with the de-selection of faulty sensels was conducted, which was based on the data obtained  
321 when loading the sensors in the pressure calibration chamber. The following experiments  
322 were then conducted:

- 323 • The sensors were loaded with a number of uniform pressures in the pressure  
324 calibration chamber (with a polythene diaphragm).
- 325 • In order to simulate the hard surface tyre loading environment, the sensors were  
326 covered with a polythene membrane and a number of individual sensing elements  
327 were randomly selected (excluding any faulty sensels) to which a range of (0 – 500 g)  
328 laboratory weights were individually applied through a 2 mm thick square rubber pad  
329 of the size of the sensor active area (Fig. 9, left and middle).
- 330 • To simulate the soil conditions, the small rubber pad was replaced with sandy loam  
331 soil confined in a 2 mm thick larger rubber pad with a central square of the same  
332 dimensions as the active area of the sensel removed. Then a range of (0 – 500 g)  
333 laboratory weights was applied to the soil placed on the selected sensels (Fig. 9,  
334 right).

335

336 The effect of the loads applied to the sensels using the three different media (polythene  
337 diaphragm, rubber pad and soil) were recorded and compared, as shown in Fig. 10 and Fig.  
338 11. The figures present data obtained for one random sensing element, as other randomly  
339 selected sensels showed similar relationships. The tests conducted in the pressure calibration  
340 chamber, using polythene diaphragm, provided data recorded by Tekscan that agree with the  
341 applied values (Fig. 10), which confirms that the data obtained when loading the sensor in the  
342 pressure calibration chamber agree with the previous calibration conducted using the same  
343 device. The relationships between the applied and recorded load, shown in Fig. 11, were  
344 found to be linear, however, the data recorded by Tekscan, when the loads were applied  
345 through the rubber pad and soil, were found to be lower than the applied load. The slopes of  
346 the relationships between the applied and measured load were found to be 0.534 and 0.567  
347 for the rubber pad and soil block, respectively. The dissimilarity is related to differences in  
348 interface material used and proved a requirement for a correction factor to be used for contact  
349 pressure tests if they were conducted using the I-Scan 9830 sensors.

350

351 b. A comparison of the load applied to tyres and recorded by the Tekscan system

352 In order to check similarity of the compliance factor during the calibration and experiments, a  
353 comparison of the weight computed from the Tekscan vertical pressure distribution and the  
354 total weight applied to a tyre, obtained by Misiewicz (2010), for the two types of Tekscan  
355 sensors was conducted.

356

357 i. I-Scan 9830 sensors

358 ~~Figure-Fig.~~ 12 presents relationships of the applied and recorded load for the tyre tested on,  
359 both, the hard surface and the soil using the I-Scan 9830 sensors. The recorded loads were  
360 less than the applied loads. The slope of the relationship between the applied and recorded  
361 load was found to be 0.639 and 0.553 on hard surface and in the soil, respectively, which was  
362 similar to the results obtained in the small scale controlled study.

363

364 ii. I-Scan 6300 sensors

365 The I-San 6300 sensors have a higher spatial resolution (active area of each sensel: 3.2 mm x  
366 2.0 mm) than the I-Scan 9830 sensors. The comparison of the loads applied to the tyres and  
367 measured by Tekscan, when testing agricultural tyres using the 6300 sensors, agreed to  
368 within  $\pm 10\%$  of the overall slope of the relationship of 0.95, as illustrated in Fig. 13.

369

370 The comparison of the load applied to tyres and measured by Tekscan sensors showed that  
371 there is a difference between the applied loads and recorded values obtained for the I-Scan  
372 9830 sensors. This difference was not found to be significant for the 6300 sensor, which has  
373 a higher spatial resolution. Therefore, this discrepancy found for the 9830 sensors was  
374 assumed to be caused by the fact that different loading materials were used for the calibration  
375 and pressure measurements. When the sensors are pressurised with air during the calibration,  
376 the pressure is uniform as the air follows the shape of Tekscan sensors. However, soil and  
377 rubber are less deformable and follow the shape of the sensors less well. As the recorded  
378 loads were considerably lower than the loads applied, it indicates that a large part of the load  
379 applied concentrated on the non-active areas of the sensors.

380

381 In order to correct the performance of Tekscan sensors in determining the contact pressure  
382 between materials different to those used in sensor calibration, all individual contact pressure  
383 data points obtained using the sensors should be increased by a correction factor calculated as  
384 applied load/recorded load for each test. This adjustment will lead to an agreement between  
385 the Tekscan recorded load and the load applied to the sensor.

386

387 Finally, the performance of Tekscan sensors in contact pressure measurements below  
388 agricultural tyres was evaluated by using the sensors for the contact pressure determination  
389 below a selection of tyres. [Figure-Fig. 14](#) presents the contact pressure profile obtained below  
390 the treadless T421 Twin Implement 600/55-26.5 tyre after the novel multi-point per sensel  
391 calibration was applied to the raw data, previously shown in [Figure-Fig. 5](#). A close  
392 agreement between the overlapping sensels in the centre of the tyre contact area was found.  
393 This indicates that the development of the new calibration procedure resulted in a significant  
394 improvement of the accuracy of the sensors and made it possible to use them to determine the  
395 pressure distribution below tyres.

396

397 [Figure-Fig. 15](#) shows an example of tyre contact pressure distribution of a Goodyear  
398 11.50/80-15.3 implement tyre on a hard surface at its recommended load of 2.18 ~~tonne~~ at  $4.1$   
399  $\times 10^5$  Pa inflation pressure. It was obtained using sensors which were previously calibrated  
400 using the multi-point per sensel calibration with sensel selection. It is recommended that this  
401 calibration procedure is used to evaluate the accuracy of the other available pressure mapping  
402 systems.

403

404 **6 Conclusions**

- 405 1. A pressure calibration chamber has shown to be a valuable tool to calibrate the  
406 sensors and to evaluate the pressure distribution of the sensors.
- 407 2. The pressure mapping sensors calibrated with the proprietary built-in calibration give  
408 the majority of bias errors below 3% and the maximum error of 12.5% when  
409 measuring the mean pressure, however, individual sensel errors of  $\pm 30\%$  were  
410 found to be present.
- 411 3. When using the multi-point per sensel calibration with sensel selection the bias errors  
412 have been reduced below 1% with both residual and statistical errors of  $\pm 4\%$  for the  
413 polynomial relationships.
- 414 4. The sensor equilibration has been found to decrease the maximum variations of  
415 Tekscan output from 130% to 6%.
- 416 5. Correction to the Tekscan output is required if the sensors are used to measure  
417 pressure between various interfaces different from those used in the calibration  
418 procedure. The compliance factor can be calculated as a ratio of applied load to load  
419 recorded by the sensor.
- 420 6. Tyre contact pressure distribution can be more confidently determined using Tekscan  
421 sensors after they are calibrated using the multi-point per sensel calibration with  
422 sensel selection, a new calibration procedure which improves the accuracy of the  
423 sensors.

424

425 **References**

- 426 Brimacombe, J., Anglin C., Hodgson A., & Wilson D. (2005). Validation of calibration  
427 techniques for Tekscan pressure sensors. Proceedings of the 20th Congress of the  
428 International Society of Biomechanics, Cleveland, OH, 31 July – 5 August 2005.
- 429 DeMarco, A.L., Rust, D.A., & Bachus, K.N. (2000). Measuring contact pressure and contact  
430 area in orthopedic applications: Fuji Film vs. Tekscan. 46<sup>th</sup> Annual Meeting of Orthopedic  
431 Research Society, Orlando, Florida, 12 – 15 March 2000.
- 432 Drewniak, E.I., Crisco, J.J., Spenciner, D.B., & Fleming, B.C. (2007). Accuracy of circular  
433 contact area measurements with thin-film pressure sensors. *Journal of Biomechanics*, 40,  
434 2569 – 2572.
- 435 Ferguson-Pell, M., Hagiwara, S., & Bain, D. (2000). Evaluation of a Sensor for Low  
436 Interface Pressure Applications. *Medical Engineering & Physics*, 22, no. 9, 657 – 663.
- 437 Horn, R., Fleige, H., Peth, S., & Peng, X. (2006). Soil management for sustainability,  
438 Advances in GeoEcology. The 17th Triennial International Soil Tillage Research Conference,  
439 CATENA VERLAG GMBH, Kiel, Germany, 28 August – 3 September 2006.

440 Maurer, J.R., Ronsky, J., Loitz-Ramage, B., Andersen, M., Zernicke, R., & Harder, J. (2003).  
441 Prosthetic socket interface pressures: Customized calibration technique for the TEKSCAN F-  
442 socket system. Summer Bioengineering Conference, Florida, 25 – 29 June 2003.

443 Misiewicz, P.A. (2010). The evaluation of the soil pressure distribution and carcass stiffness  
444 resulting from pneumatic agricultural tyres, PhD Thesis, Cranfield University.

445 Soane, B.D., & Ouwerkerk, C. (1994). Soil compaction problems in word agriculture. In B.  
446 D. Soane, & C. Ouwerkerk (Eds). *Soil compaction in crop production* (pp. 1-21). The  
447 Netherlands: Elsevier Science.

448 Sumiya, T., Suzuki, Y., Kasahara, T., & Ogata, H. (1998). Sensing stability and dynamic  
449 response of the F-scan in-shoe sensing system: A technical note. *Journal of Rehab. Res.*  
450 *Devel.*, 35, 192 – 200.

451 Tekscan. (2006). Tekscan I-Scan User Manual, Tactile force and pressure measurements  
452 system, v. 5.8x, published by Tekscan Inc, South Boston, Mass., USA.

453 Tekscan. (not dated a). Tekscan home page, available at: [www.tekscan.com](http://www.tekscan.com) (accessed on 15  
454 June 2013).

455 Tekscan (not dated b). Tekscan technology, available at: [http://www.tekscan.com/tekscan-  
456 technology](http://www.tekscan.com/tekscan-technology) (accessed on 1 April 2014).

457 Wilson, D.C., Niosi, C.A., Zhu, Q.A., Oxland T.R., & Wilson, D.R. (2006). Accuracy and  
458 repeatability of a new method for measuring facet loads in the lumbar spine. *Journal of*  
459 *Biomechanics*, 39, 348 – 353.

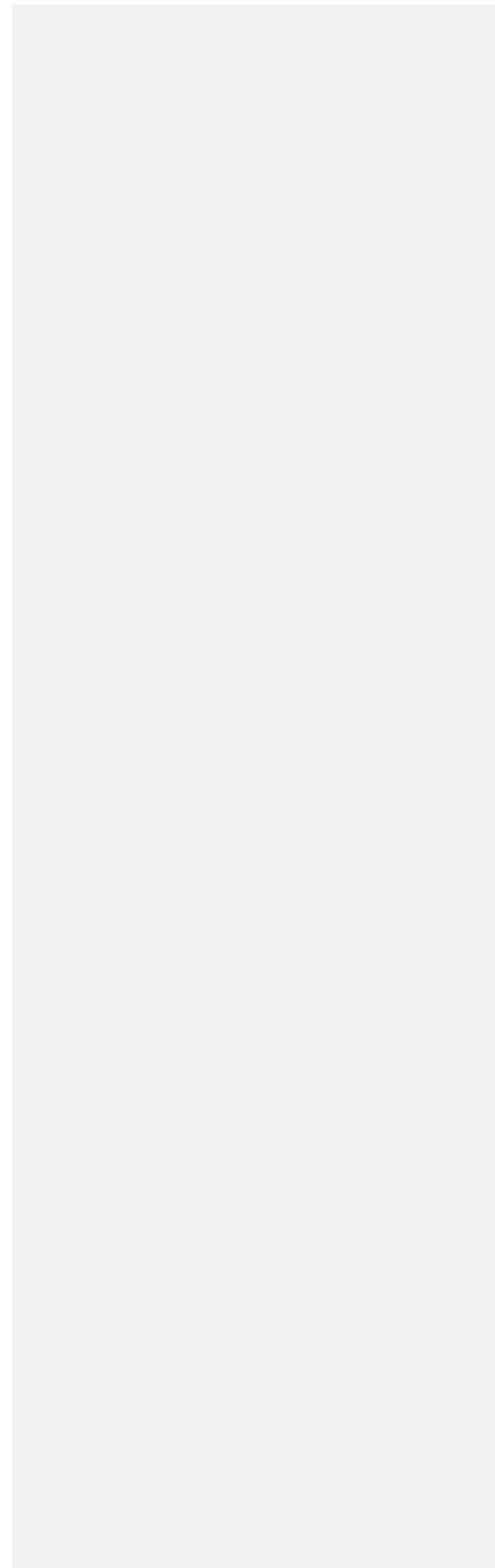
460 Wilson, D.R., Apreleva, M.V., Eichler, M.J., & Harrold, F.R. (2003). Accuracy and  
461 repeatability of a pressure measurement system in the patellofemoral joint. *Journal of*  
462 *Biomechanics*, 36, 1909 – 1915.

463

464  
465 **Figures:**  
466 Fig. 1 – Tekscan pressure mapping sensors (from left: Conformat model 5330 sensor, I-Scan  
467 model 6300 sensors, I-Scan model 9830 sensors)  
468 Fig. 2 – Pressure calibration chamber  
469 Fig. 3 – Cross section of the pressure calibration chamber showing the individual components  
470 Fig. 4 – Residual error histograms for the 5 Tekscan sensors calibrated using the Tekscan  
471 proprietary calibration (please note vertical scales are different between the five sub-figures)  
472 Fig. 5 – Cross sectional profiles of tyre contact pressure obtained below a smooth Trelleborg  
473 T421 Twin Implement 600/55-26.5 tyre using I-Scan 9830 sensors; a: non-calibrated and  
474 non-equilibrated data; b: data calibrated and equilibrated following Tekscan procedure.  
475 Dashed ovals indicate the results obtained by overlapping sensels  
476 Fig. 6 – Pressure applied vs. output for each sensing element of the I-Scan 9830-A sensor  
477 (top: non-calibrated and non-equilibrated data, bottom: non-calibrated but equilibrated data)  
478 Fig. 7 – Residual errors for the I-Scan 9830-A sensor after multi-point per sensel calibration;  
479 a: linear, b: power, c: 2<sup>nd</sup>, d: 3<sup>rd</sup> and e: 4<sup>th</sup> order polynomial (please note horizontal and  
480 vertical scales are different between the five sub-figures)  
481 Fig. 8 – Statistical errors for I-Scan 9830-A sensor after the multi-point per sensel calibration;  
482 a: linear, b: power, c: 2<sup>nd</sup>, d: 3<sup>rd</sup> and e: 4<sup>th</sup> order polynomial (please note horizontal and  
483 vertical scales are different between the five sub-figures)  
484 Fig. 9 – Small scale controlled study on the I-Scan 9830 sensors (left and middle: rubber pad  
485 tests, right: soil test)  
486 Fig. 10 – Measured vs. applied load for I-Scan 9830-A sensor loaded in the pressure  
487 calibration chamber using a polythene diaphragm  
488 Fig. 11 – Measured vs. applied load for I-Scan 9830-A sensor; left: load applied through a  
489 rubber pad, right: load applied through soil (1:1 line dashed)  
490 Fig. 12 – Measured vs. applied load for I-Scan 9830 sensors when loaded by the T421 Twin  
491 Implement 600/55-26.5 tyre; left: hard surface, right: soil (1:1 line dashed)  
492 Fig. 13 – Measured vs. applied load for I-Scan 6300 sensor when loaded by an 11.50/80–15.3  
493 implement tyre on the hard surface (1:1 line dashed)  
494 Fig. 14 – Cross sectional profile of tyre contact pressure below the treadless T421 Twin  
495 Implement 600/55-26.5 tyre obtained using I-Scan 9830 sensors; data calibrated and  
496 equilibrated according to the multi-point per sensel calibration. Dashed ovals indicate the  
497 results obtained by overlapping sensels



498 Fig. 15 – A Goodyear 11.50/80–15.3 implement tyre at 2.18 ~~tonne~~ load and  $4.1 \times 10^5$  Pa  
499 inflation pressure; left: tyre tread pattern; right: tyre contact pressure distribution ( $10^5$  Pa)  
500 obtained using the multi-point per sensel calibration with sensel selection (direction of travel:  
501 from right to left)  
502  
503



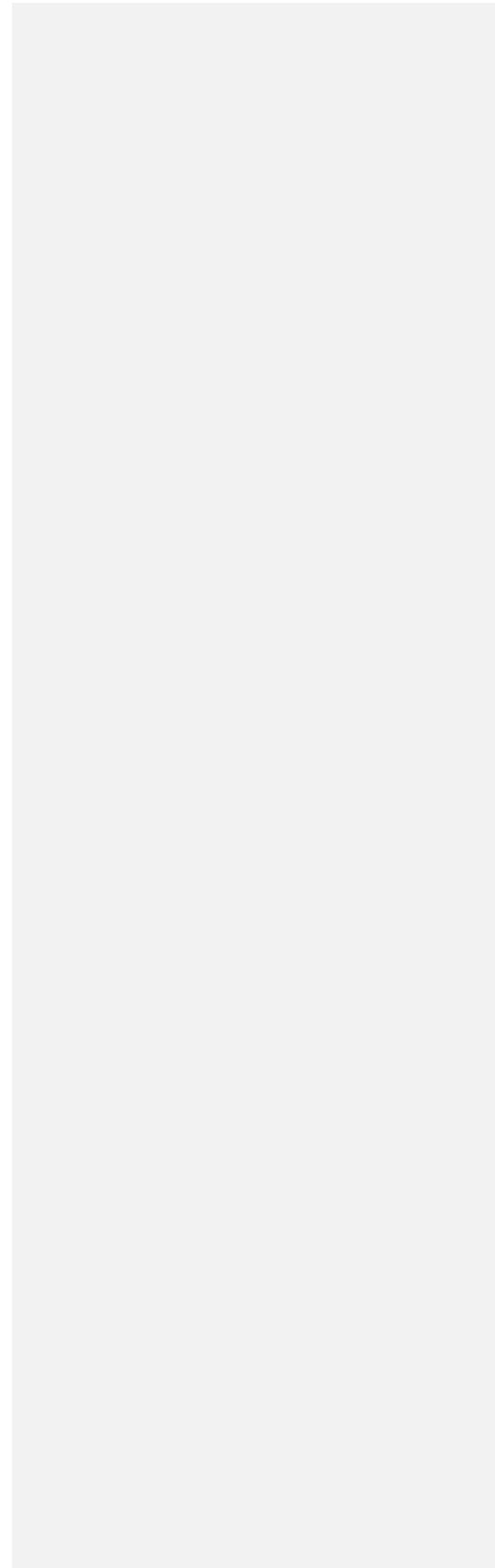
504

505 **Table:**

506 Table 1 – Pressure and bias error results based on the Tekscan proprietary calibration

507

508



509



510

511 Fig. 1

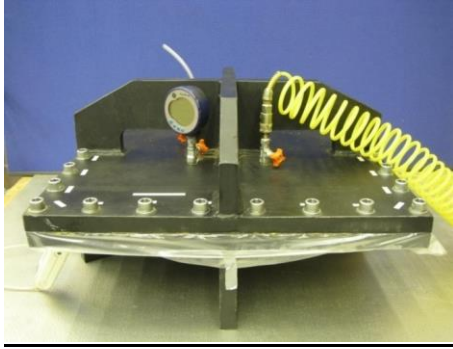
512 Tekscan pressure mapping sensors (from left: Conformat model 5330 sensor, I-Scan model

513 6300 sensors, I-Scan model 9830 sensors)

514

515

516



517

518 Fig. 2

519 Pressure calibration chamber

520

521

522

523

524

525

526

527

528

529

530

531

532

533

534

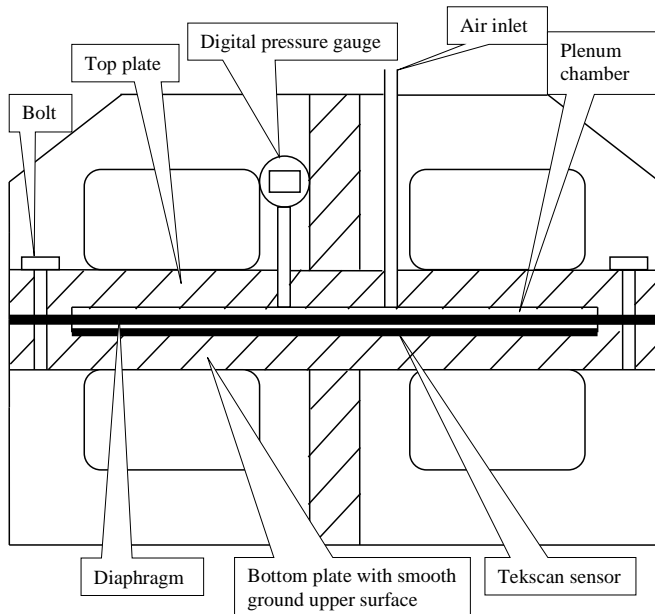
535

536

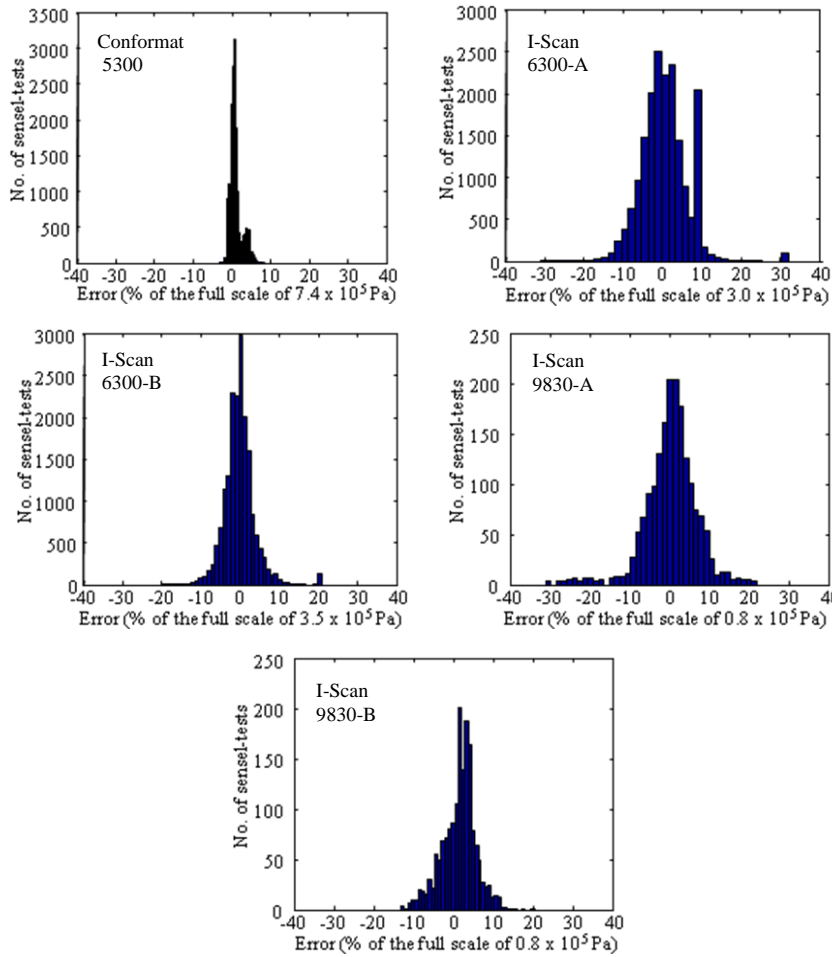
537 Fig. 3

538 Cross section of the pressure calibration chamber showing the individual components

539



540



541

542

543

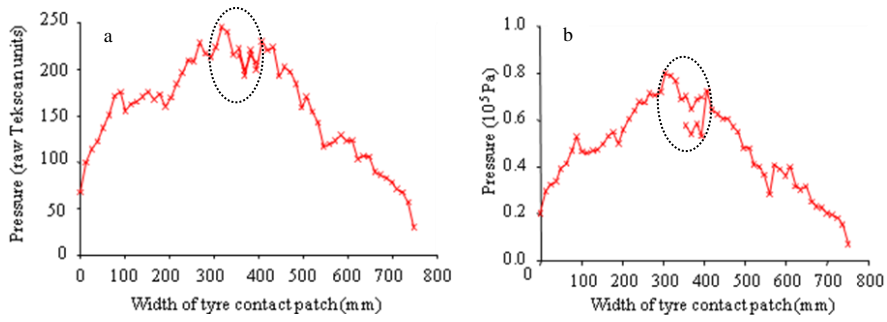
544 Fig. 4

545 Residual error histograms for the 5 Tekscan sensors calibrated using the Tekscan proprietary  
546 calibration (please note vertical scales are different between the five sub-figures)

547

548

549



550

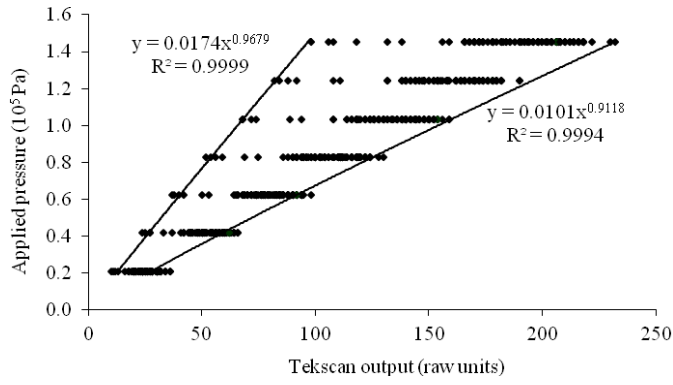
551 Fig. 5

552 Cross sectional profiles of tyre contact pressure obtained below a smooth Trelleborg T421  
553 Twin Implement 600/55-26.5 tyre using I-Scan 9830 sensors; a: non-calibrated and non-  
554 equilibrated data; b: data calibrated and equilibrated following Tekscan procedure. Dashed  
555 ovals indicate the results obtained by overlapping sensels

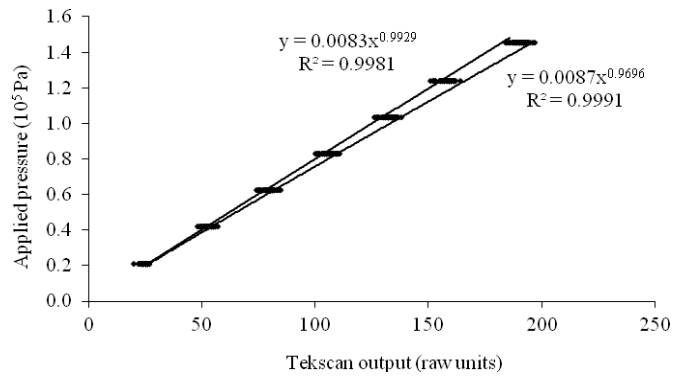
556

557

558



559



560

561 Fig. 6

562 Pressure applied vs. output for each sensing element of the I-Scan 9830-A sensor (top: non-

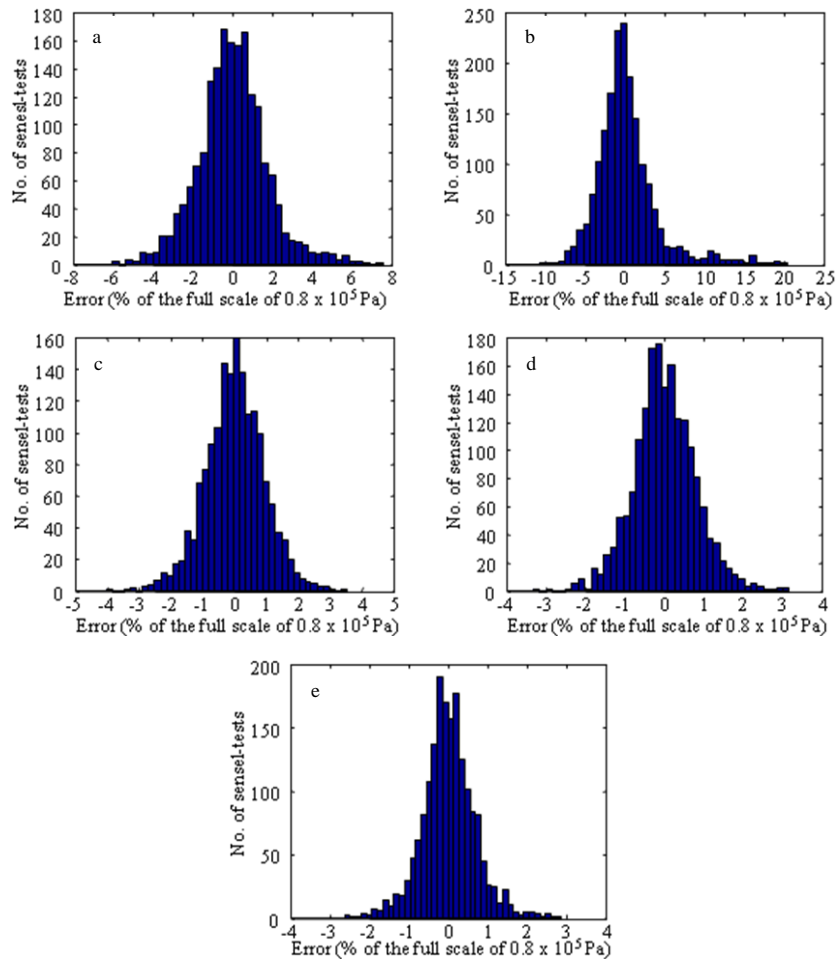
563 calibrated and non-equilibrated data, bottom: non-calibrated but equilibrated data)

564



565

566



567

568

569

570 Fig. 7

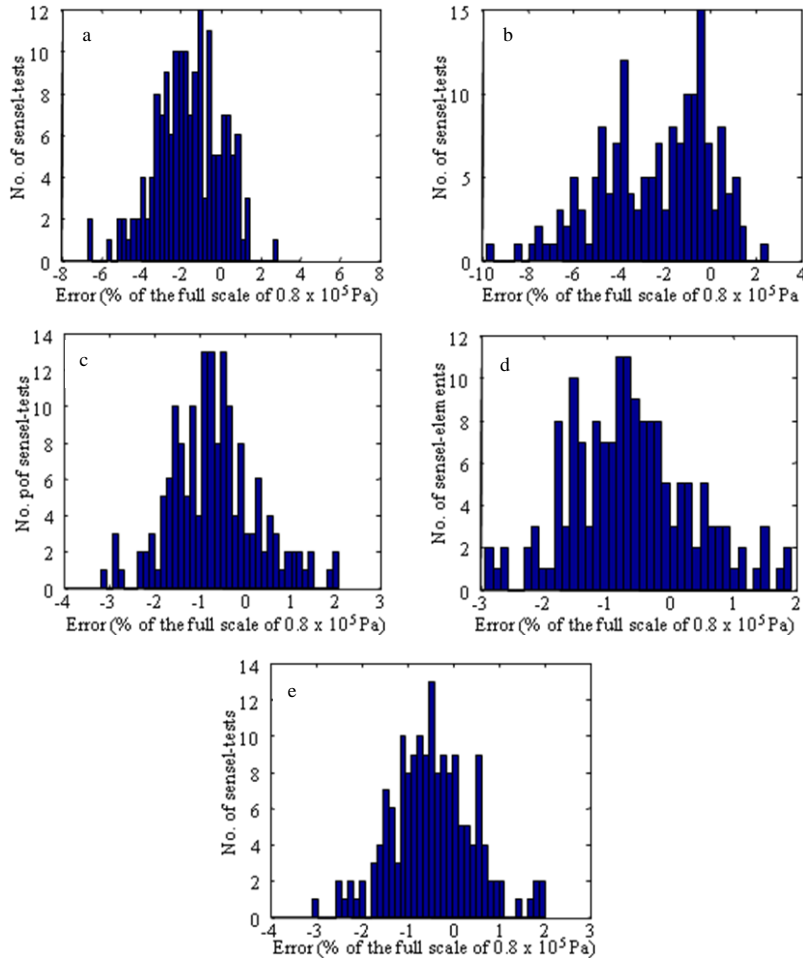
571 Residual errors for the I-Scan 9830-A sensor after multi-point per sensel calibration; a: linear,

572 b: power, c: 2<sup>nd</sup>, d: 3<sup>rd</sup> and e: 4<sup>th</sup> order polynomial (please note horizontal and vertical scales

573 are different between the five sub-figures)

574

575



576

577

578

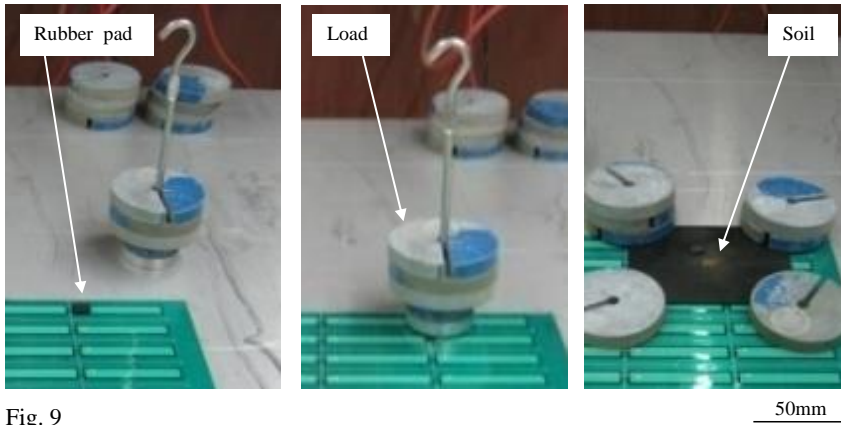
579 Fig. 8

580 Statistical errors for I-Scan 9830-A sensor after the multi-point per sensel calibration; a:  
581 linear, b: power, c:  $2^{\text{nd}}$ , d:  $3^{\text{rd}}$  and e:  $4^{\text{th}}$  order polynomial (please note horizontal and vertical  
582 scales are different between the five sub-figures) [figure 8](#)

583

584

585



586

587 Fig. 9

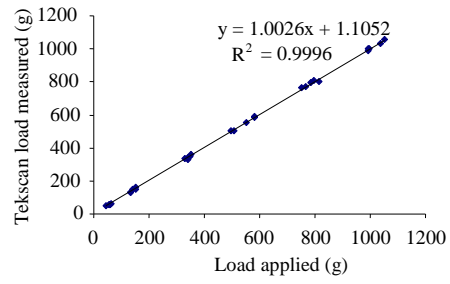
588 Small scale controlled study on the I-Scan 9830 sensors (left and middle: rubber pad tests,

589 right: soil test)

590

591

592



593

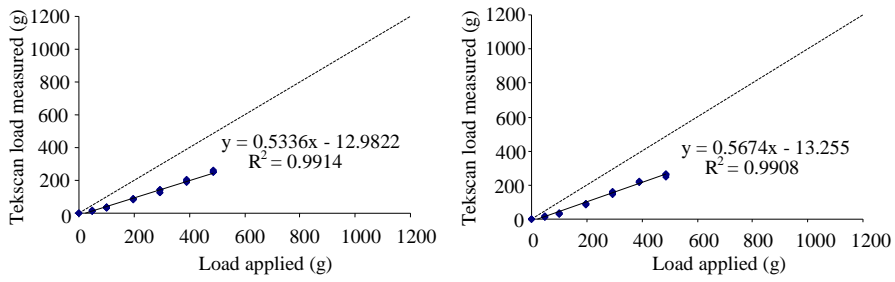
594 Fig. 10

595 Measured vs. applied load for I-Scan 9830-A sensor loaded in the pressure calibration

596 chamber using a polythene diaphragm

597

598



600

601 Fig. 11

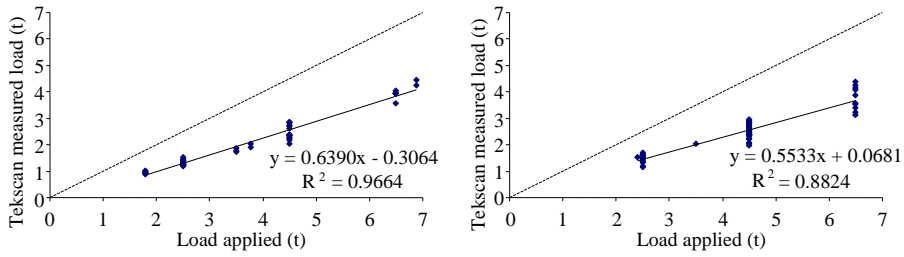
602 Measured vs. applied load for I-Scan 9830-A sensor; left: load applied through a rubber pad,

603 right: load applied through soil (1:1 line dashed)

604

605

606



607

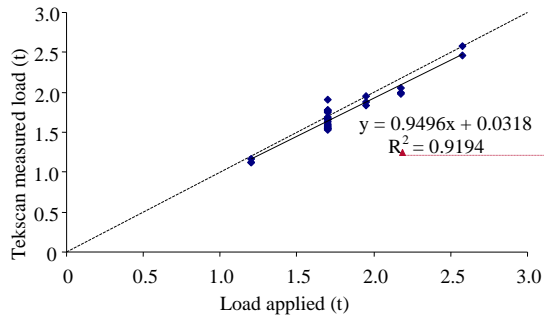
608 Fig. 12

609 Measured vs. applied load for I-Scan 9830 sensors when loaded by the T421 Twin Implement

610 600/55-26.5 tyre-; left: hard surface, right: soil (1:1 line dashed)

611

612



Formatted: Superscript

613

614 Fig. 13

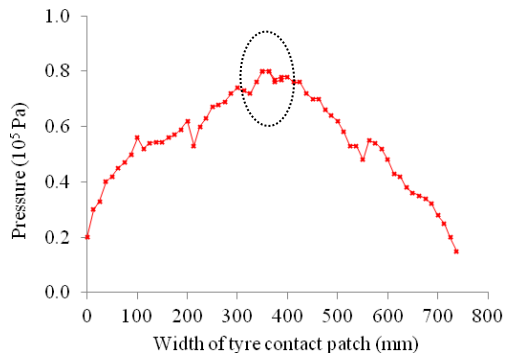
615 Measured vs. applied load for I-Scan 6300 sensor when loaded by an 11.50/80-15.3

616 implement tyre on the hard surface (1:1 line dashed)

617

618

619



620

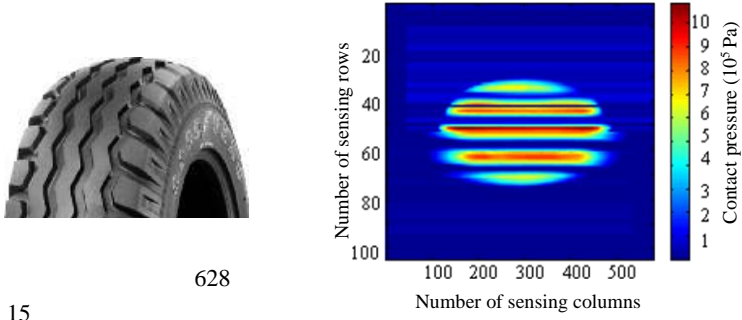
621 Fig. 14

622 Cross sectional profile of tyre contact pressure below the treadless T421 Twin Implement  
623 600/55-26.5 tyre obtained using I-Scan 9830 sensors; data calibrated and equilibrated  
624 according to the multi-point per sensel calibration. Dashed ovals indicate the results obtained  
625 by overlapping sensels

626



627



629 Fig. 15

630 A Goodyear 11.50/80-15.3 implement tyre at 2.18 tonne load and  $4.1 \times 10^5$  Pa inflation  
631 pressure; left: tyre tread pattern; right: tyre contact pressure distribution ( $10^5$  Pa) obtained  
632 using the multi-point per sensel calibration with sensel selection (direction of travel: from  
633 right to left)

634

635

636

637 Table 1

638 Pressure and bias error results based on the Tekscan proprietary calibration

Sensor	Pressure applied (10 <sup>5</sup> Pa)	Tekscan results			Bias error <sup>1</sup> (%)
		Mean pressure (10 <sup>5</sup> Pa)	Maximum pressure (10 <sup>5</sup> Pa)	Minimum pressure (10 <sup>5</sup> Pa)	
Conformat 5330	0.689	0.669	0.756	0.559	-2.9
	1.386	1.395	1.498	1.282	+ 0.6
	2.101	2.164	2.392	2.015	+ 3.0
	2.759	2.805	3.343	1.903	+ 1.7
I-Scan 6300-A	0.689	0.705	1.231	0.307	+ 2.2
	1.379	1.385	1.988	0.635	+ 0.5
	2.068	2.059	3.019	1.206	- 0.4
	2.758	2.789	3.019	1.822	+ 1.1
I-Scan 6300-B	0.689	0.678	0.916	0.394	- 1.6
	1.379	1.381	1.626	1.157	+ 0.2
	2.068	2.050	2.424	1.804	- 0.9
	2.758	2.730	3.485	2.344	- 1.0
I-Scan 9830-A	0.138	0.132	0.196	0.084	- 4.0
	0.276	0.256	0.298	0.221	- 7.3
	0.414	0.440	0.478	0.407	+ 6.3
	0.552	0.621	0.716	0.600	+ 12.5
I-Scan 9830-B	0.138	0.145	0.233	0.090	+ 5.5
	0.276	0.265	0.303	0.230	- 4.0
	0.414	0.385	0.414	0.354	- 6.8
	0.552	0.557	0.563	0.495	+ 1.0

639

640

<sup>1</sup> Bias error (%) was calculated as 100% × (Mean pressure - Pressure applied)/(Pressure applied).